



Crystal structure and characterization of L-arginine chlorate and L-arginine bromate[☆]

A.M. Petrosyan^{a,*}, H.A. Karapetyan^a, R.P. Sukiasyan^a, A.E. Aghajanyan^b,
V.G. Morgunov^c, E.A. Kravchenko^c, A.A. Bush^d

^aMolecule Structure Research Center, NAS, 26 Azatutyan Ave., Yerevan 375014, Armenia

^bInstitute of Biotechnology, 14 Gyurjyan St., Yerevan 375056, Armenia

^cInstitute of General and Inorganic Chemistry, RAS, 31 Leninskii pr., Moscow 123812, Russia

^dMoscow State Institute of Radioengineering, Electronics and Automation, 78 Vernadskii St., Moscow 119454, Russia

Received 17 January 2005; revised 25 May 2005; accepted 25 May 2005

Available online 20 July 2005

Abstract

The salts L-arginine.HClO₃ and L-arginine.HBrO₃ were synthesized. The crystals obtained were characterized by IR and NQR spectroscopy, thermal analysis, Nd:YAG laser radiation second harmonic generation, dielectric, piezoelectric and pyroelectric measurements and their crystal structures were determined. L-arginine.HClO₃ and L-arginine.HBrO₃ are crystallized in orthorhombic (space group P2₁2₁2₁) and triclinic (space group P1) systems, respectively. Their structures consist of the protonated arginine cation [⁺(H₂N)₂CNH(CH₂)₃.CH(NH₃⁺)COO⁻] and respective ClO₃⁻ or BrO₃⁻ anions. Hydrogen bonds (stronger in the bromate) connect anions with cations and the latter with each other. However, these salts have essential distinctions in crystal packing.

© 2005 Elsevier B.V. All rights reserved.

Keywords: L-Arginine chlorate; Bromate; Crystal structure; Solution growth; Properties

1. Introduction

L-Arginine phosphate monohydrate L-Arg.H₃PO₄.H₂O (LAP) is one of the best nonlinear optical crystals [1]. However, growth of the LAP crystals has attendant growth of microorganisms, which can be detrimental to crystal quality. Hence, the preparation procedure requires special precautions. It has been suggested that the appearance of microorganisms can be prevented by either adding H₂O₂ [2] or Hg [3] into solution or by covering the solution with a layer of n-hexane [4]. Ongoing investigations [5–9], however, showed that this does not completely solve the problem. Search for new members of the LAP family may

produce crystals, whose parameters can surpass those of the LAP. In addition, the preparation of such crystals may be free of the problem of microorganisms [10–13]. Systematic search for new LAP-analogs was started by Monaco et al. [14], who investigated some previously known and a number of new crystals. The interaction of L-arginine with iodic acid only, among the halogenic acids HClO₃, HBrO₃, HIO₃, was investigated to give powdered L-Arg.HIO₃. The weak broad iodine-127 lines were observed in the nuclear quadrupole resonance (NQR) spectrum [15], which to a certain extent, was evidence for the crystallinity of the compound. In addition, it was found that L-Arg.2HIO₃ comprising a doubly charged arginine cation [⁺(H₂N)₂.CNH(CH₂)₃.CH(NH₃⁺)COOH] exists, which, in contrast to L-Arg.HIO₃ crystallizes easily [15]. In this respect, we found it interesting to study the possibility of formation and crystallization of the respective salts of L-arginine with chloric (HClO₃) and bromic (HBrO₃) acids.

2. Experimental

As initial compounds, we used L-arginine, synthesized in the Institute of Biotechnology (Yerevan), and a reagent

[☆] CCDC 259335 and CCDC 259336 contain the supplementary crystallographic data for this paper. These data can be obtained free of charge via www.ccdc.cam.ac.uk/conts/retrieving.html (or from the Cambridge Crystallographic Data Centre, 12 Union Road, Cambridge CB2 1EZ, UK; fax: +44 1223 336033).

* Corresponding author. Tel.: +374 1 281764; fax: +374 1 282267.

E-mail address: apetros@msrc.am (A.M. Petrosyan).

purchased from «Sigma» Chemical Company. For preparation of HClO_3 and HBrO_3 , we used, respectively, KClO_3 and $\text{Ba}(\text{BrO}_3)_2 \cdot \text{H}_2\text{O}$, both of reagent grade. The IR spectra were registered using Specord 75 IR spectrophotometer (Carl Zeiss, Jena) by the technique of nujol mull suspension ($4000\text{--}400\text{ cm}^{-1}$) and Nicolet 'Nexus' FT-IR spectrometer with ZnSe prism ($4000\text{--}650\text{ cm}^{-1}$). The thermal properties were studied using a Paulik-Paulik- Erdey Derivatograph (type 3427–904) and a Boetius-type microscope. The nuclear quadrupole resonance (NQR) spectra were measured using a pulse NQR spectrometer operating within 2–300 MHz.

The measurements of dielectric constant ϵ and the tangent of the loss $\tan\delta$ were performed by means of the ac bridge P5083 at the frequency of measuring field 1 kHz. The piezoelectric effect in crystals was induced by alternating mechanical load. The sample was sandwiched between the faces of two vertical metallic rods, and 0.7 kHz longitudinal oscillations were generated using a piezoelectric transducer. The resulting charge is proportional to the piezoelectric charge coefficient d'_{33} and gives rise to an A.C. voltage. The installation was calibrated using X-cut quartz plates. The pyroelectric measurements were carried out by the quasi-static method. The pyroelectric constant γ was calculated by formula $\gamma = I/[S(dT/dt)]$, where I is the pyroelectric current measured in a circuit sample-electrometer (V7-30) during uniform change of the sample's temperature with the rate of $dT/dt \sim 0.1$ grad/sec, S is the area of the Ag electrodes on the base surfaces of the sample. The dielectric, piezoelectric and pyroelectric measurements were performed on single crystal plates with ~ 1 mm thickness and $S \sim 5\text{ mm}^2$ for L-Arg.HClO_3 and $S \sim 50\text{ mm}^2$ for L-Arg.HBrO_3 . In order to prepare electrodes the base surfaces of plates were coated by silver paste. The orientations of the crystallographic axes for the crystals were determined by X-ray studies on a DRON-4 diffractometer. X-ray diffraction data for structure solution

were collected using CAD-4 automatic diffractometer (ENRAF NONIUS). The structures were determined by the direct method and refined using the SHELX86 and SHELXL93 programs [16,17].

3. Results and discussions

3.1. Synthesis, growth and characterization of crystals

Chloric and bromic acids (unlike iodic) exist only as dilute solutions. The solution of HClO_3 was obtained by passing an aqueous solution of KClO_3 through an exchange column with sulphocationite KU-2-8 in H^+ form. The solution of HBrO_3 was obtained after precipitation and isolation of barium sulphate by the reaction



Then the solution of L-arginine was added to the HClO_3 and HBrO_3 solutions to obtain mixtures with required L-Arg: acid ratios. Crystallization was reached by slow evaporation of the solutions at room temperature. The crystals L-Arg.HClO_3 and L-Arg.HBrO_3 were grown from aqueous solutions with equimolar L-Arg: acid ratio. No crystals were obtained from the solutions with 1:2 and 1:3 ratios. If the concentration of the above solutions increased, the HBrO_3 -system decomposed and that with HClO_3 exploded, probably because of instability of HClO_3 and HBrO_3 at high concentrations. Using spontaneously formed crystals as the seeds and evaporating small volumes of solutions at room temperature, we obtained single crystals of L-Arg.HBrO_3 , which measured $13 \times 11 \times 6\text{ mm}^3$, and L-Arg.HClO_3 of $28 \times 8 \times 7\text{ mm}^3$ in size. These crystals were used for measurements of physical properties. The crystals of L-Arg.HClO_3 were of optical quality. No microorganisms appeared in the solutions during crystallization.

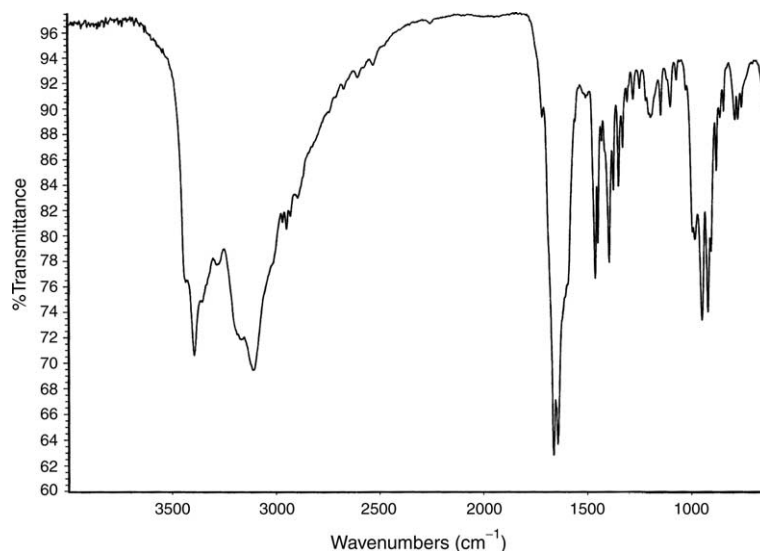


Fig. 1. ATR FTIR spectrum of $\text{L-Arg} \cdot \text{HClO}_3$ crystals.

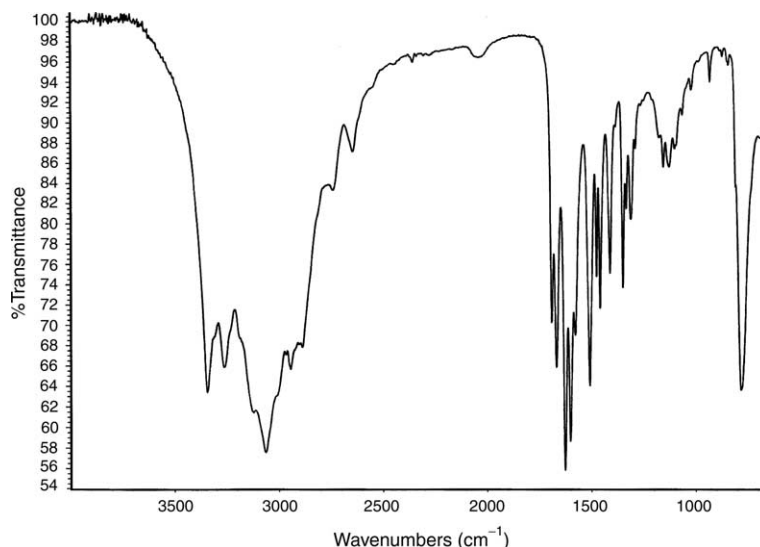


Fig. 2. ATR FTIR spectrum of L-Arg·HBrO₃ crystals.

The crystals of L-arginine chlorate and bromate were expected to form via singly-charged cation L-ArgH⁺ (or L-Arg⁺), namely, ⁺[(H₂N)₂CNH](CH₂)₃CH(NH₃⁺)COO⁻ and the respective ClO₃⁻ and BrO₃⁻ anions, which is the usual mechanism for salts of 1:1 composition. The IR and NQR spectra are in accordance with this expectation. The IR spectra are shown in Figs. 1 and 2. Comparison of the IR spectrum for L-Arg.HClO₃ with that for KClO₃ enables one to assign the absorption band at 900–1000 cm⁻¹ to the stretching (ν_1, ν_3) vibration of Cl–O bonds in the ClO₃⁻ ion (920.37 cm⁻¹, 949.46 cm⁻¹). The respective bands of deformation vibrations (not shown in Fig. 1) are at 603 cm⁻¹ (ν_2) and 487 cm⁻¹ (ν_4). The absorption bands of ν (N–H) stretching vibrations of guanidyl and NH₃⁺ groups are at 3000–3500 cm⁻¹ (3111.71 cm⁻¹, 3168.01 cm⁻¹, 3284.02 cm⁻¹, 3392.42 cm⁻¹, 3432.70 cm⁻¹). The absorption band with peaks at 1663.29 cm⁻¹ and 1642.79 cm⁻¹ correspond to asymmetric stretching vibration of carboxylate group and deformation vibration of NH₂⁺ and NH₃⁺ groups. Similar absorption bands of L-Arg⁺ can also be found in the spectrum of L-Arg.HBrO₃. The strong band near 800 cm⁻¹ (783.93 cm⁻¹ and 809.15 cm⁻¹) represents absorption caused by the stretching vibrations of Br–O bonds in the BrO₃⁻ ion. A similar absorption band with the same number of peaks was observed in the same region of the spectrum of Ba(BrO₃)₂·H₂O. In the region of the ν (N–H) stretching vibrations there are peaks at 3065.04 cm⁻¹, 3122.70 cm⁻¹, 3263.13 cm⁻¹ and 3343.75 cm⁻¹. Decrease in the ν (N–H) stretching vibration frequencies in the spectrum of L-Arg.HBrO₃ compared to L-Arg.HClO₃ is probably caused by stronger N–H···O hydrogen bonds in L-arginine bromate. In the range of 1700–1550 cm⁻¹, there is a strong absorption band with peaks at 1692.50 cm⁻¹, 1670.23 cm⁻¹, 1627.48 cm⁻¹, 1602.34 cm⁻¹ and 1579.12 cm⁻¹. An increase in the vibration frequencies of

the carboxylate group COO⁻ (1692.50 cm⁻¹ and 1670.23 cm⁻¹) may result from the difference in the C–O bond lengths due to hydrogen bond formation [15].

The L-Arg.HClO₃ and L-Arg.HBrO₃ crystals were also studied using ³⁵Cl and ⁷⁹Br nuclear quadrupole resonances (NQR). Table 1 lists the measured frequencies and relaxation times of the resonant lines at 77 K. The NQR spectrum of L-Arg.HClO₃ consists of a strong singlet, and that of L-Arg.HBrO₃ - of a strong, well-resolved doublet. The intensity of resonant lines, however, rapidly decreased with increasing temperature, and at room temperature, the signals were not observed. As evidenced by the number of resonant lines at 77 K, all the ClO₃⁻ ions are crystallographically equivalent in the unit cell of L-Arg.HClO₃, while in the unit cell of L-Arg.HBrO₃ two non-equivalent BrO₃⁻ ions are present. Thus L-Arg.HClO₃ and L-Arg.HBrO₃ are not isostructural. The ³⁵Cl and ⁷⁹Br NQR frequencies are characteristic for the ClO₃⁻ and BrO₃⁻ ions and close to the ³⁵Cl and ⁷⁹Br NQR frequencies for initial KClO₃ and Ba(BrO₃)₂·H₂O (28.954 MHz and 176.223 MHz, respectively) [18].

On heating L-Arg.HClO₃ melts at 170 °C, and above 180 °C the compound begins to decompose with an exothermal effect. L-Arg.HBrO₃ decomposes at a lower temperature (145 °C). Both crystal forms were checked for the second harmonic generation (Nd:YAG laser), and in the higher quality L-Arg.HClO₃ crystal a strong phase-matched second harmonic generation signal was observed.

Table 1
³⁵Cl and ⁷⁹Br NQR frequencies and relaxation times at 77 K

Crystals	$\nu(\pm 1/2 \rightarrow \pm 3/2)$, MHz	T_1 , ms	T_2 , μ s
L-Arg·HClO ₃	29.948(7)	270	1100
L-Arg·HBrO ₃	175.69(2)	12	230
	175.99(2)	14	280

Table 2

The Miller indexes (*hkl*) of basic plane of the studied crystals, dielectric constant ϵ , dielectric loss $\tan \delta$, piezoelectric d'_{33} and pyroelectric γ coefficients at room temperature

Crystals	(<i>hkl</i>)	ϵ	$\tan \delta$	d'_{33} , 10^{-12} C/N	γ , nC/ cm^2 K
L-Arg·HClO ₃	(020)	5.1	0.019	0.70	$<4.0 \cdot 10^{-3}$
L-Arg·HBrO ₃	(1–10)	3.3	0.010	0.32	0.60

The results of dielectric, piezoelectric and pyroelectric measurements of crystals are presented in Table 2 and Fig. 3. The L-Arg.HBrO₃ crystal exhibits a rather strong pyroelectric effect in accordance with its polar symmetry P1. The temperature dependencies of the dielectric constant and dielectric loss of these crystals show smooth changes without any anomaly in the 100–400 K temperature range (Fig. 3). The temperature dependence of the pyroelectric constant is also smooth in the 125–360 K range. The rather sharp increase of apparent pyroelectric signal at $T > 360$ K and its maximum at 375 K are evidently caused by the appearance of thermostimulated currents in this temperature range. In the temperature range 125–360 K the measured signal changes its sign upon switching from heating to cooling of the sample and on the contrary, at $T > 360$ K the sign of signal does not depend on regime of the temperature change.

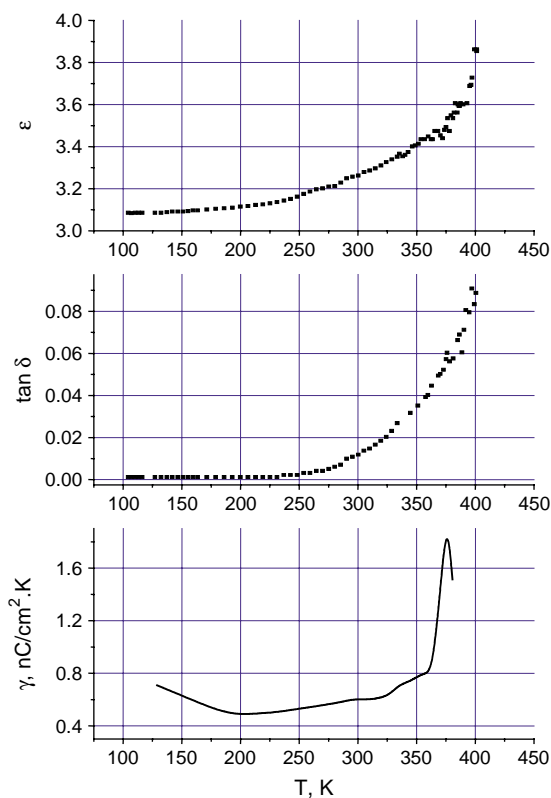


Fig. 3. Temperature dependencies of dielectric constant ϵ , dielectric loss $\tan \delta$ and pyroelectric coefficient γ measured perpendicular to (1–10) plane of L-Arg·HBrO₃ single crystals.

3.2. Crystal structure of L-Arg.HClO₃ and L-Arg.HBrO₃

The crystal structure of L-arginine chlorate was determined at room temperature, and that of L-arginine bromate, at 233 K. The crystal data and additional information on the determination of both structures are presented in Table 3. The hydrogen atoms positions were determined from the difference electron density synthesis. The chlorate and bromate of L-arginine are not isostructural. L-Arg.HClO₃ crystallizes in orthorhombic space group P2₁2₁2₁ with Z=4, while L-Arg.HBrO₃, in triclinic space group P1 with Z=2. Figs. 4 and 5 show the independent parts of the unit cells of the crystals. Packing in the crystal structures are shown in the Figs. 6 and 7. Bonds lengths and angles are presented in Tables 4 and 5, and hydrogen bond parameters in Tables 6 and 7.

As one can see from Figs. 4 and 5, the formation mechanism of L-arginine chlorate and bromate is common for salts of 1:1 composition. In the singly charged L-Arg⁺ cation, guanidyl and α -amino groups are protonated at the expense of protons of the respective acids (HClO₃ and HBrO₃) and deprotonation of their own carboxyl group. The presence of positively charged guanidyl and α -amino groups and negatively charged carboxylate group in the L-Arg⁺ cation, results in interaction of neighboring cations via N–H···O hydrogen bonds between guanidyl and carboxylate groups in crystalline salts of arginine. This interaction takes place in both structures. However, the detailed comparison revealed essential differences in interactions between cations in both structures, in cation conformations and also in their interactions with anions. As can be seen from Figs. 5 and 7, two crystallographically independent cations in the structure of L-arginine bromate are connected with each other through hydrogen bonds between N(3) and N(4) atoms of guanidyl groups and oxygen atoms of carboxylate groups. This type of interaction was designated by Salunke and Vijayan as type A [19]. Arginine cations form a kind of dimer. These dimers are connected with each other by stronger H-bonds between protonated α -amino groups N(1A) and N(1B), accordingly, and oxygen atoms O(2B) and O(2A) (compare H···O distances in the N(1)–H···O(2) hydrogen bonds with respective distances in the N(3)–H···O(2) and N(4)–H···O(1) hydrogen bonds). This leads to lengthening of the C(1)–O(2) bonds in both carboxylate groups in comparison with the C(1)–O(1) bonds (Table 5). The essential distinction in bond lengths of C(1)–O(1) and C(1)–O(2) can explain an increase of asymmetric stretching vibration frequencies of COO[−] groups (Fig. 2). The aforementioned dimers form layers parallel to the diagonal (110) plane (Fig. 7).

In the structure of L-arginine chlorate the cations interact in a different way (Fig. 6). O(1) and O(2) oxygen atoms of the carboxylate group form H-bonds with N(3) and N(2) nitrogen atoms, respectively. This type of interaction was designated as type B [19]. At the same time, the O(1) atom

Table 3
Crystal data and structure refinement for L-Arg·HClO₃, L-Arg·HBrO₃

Empirical formula	C ₆ H ₁₅ ClN ₄ O ₅	C ₆ H ₁₅ BrN ₄ O ₅
Formula weight	258.67	303.13
Temperature	293 K	233 K
Wavelength, Å	0.71073	0.71073
Crystal system	Orthorhombic	Triclinic
Space group	P2 ₁ 2 ₁ 2 ₁	P1
Unit cell dimensions	$a = 5.1928(10)$ Å, $\alpha = 90^\circ$, $b = 13.852(3)$ Å, $\beta = 90^\circ$, $c = 15.734(3)$ Å, $\gamma = 90^\circ$	$a = 8.426(2)$ Å, $\alpha = 111.05(3)^\circ$, $b = 8.737(2)$ Å, $\beta = 99.43(3)^\circ$, $c = 9.301(2)$ Å, $\gamma = 110.90(3)^\circ$
Volume, Z	1131.8 Å ³ , 4	562.5(2) Å ³ , 2
Density (calculated)	1.518 Mg/m ³	1.790 Mg/m ³
Density (measured)	1.518(2) Mg/m ³	1.77(2) Mg/m ³
Absorption coefficient	0.352 mm ⁻¹	3.669 mm ⁻¹
$F(000)$	544	308
Crystal size (mm)	0.28 × 0.21 × 0.1	0.28 × 0.21 × 0.08
θ range for data collection	1.96–27.96°	2.49–25.97°
Limiting indices	0 ≤ h ≤ 6, 0 ≤ k ≤ 18, 0 ≤ l ≤ 20	−9 ≤ h ≤ 10, −10 ≤ k ≤ 10, −10 ≤ l ≤ 11
Reflections collected	1615	2441
Independent reflections	1595 ($R_{int} = 0.0000$)	2301 ($R_{int} = 0.0000$)
Absorption correction	None	None
Refinement method	Full-matrix least-squares on F^2	Full-matrix least-squares on F^2
Data/restraints/parameters	1352/0/191	2297/3/290
Goodness-of-fit on F^2	1.055	1.107
Final R indices [$I > 2\sigma(I)$]	$R1 = 0.0349$, $wR2 = 0.0915$	$R1 = 0.0461$, $wR2 = 0.1106$
R indices (all data)	$R1 = 0.0349$, $wR2 = 0.0915$	$R1 = 0.0464$, $wR2 = 0.1106$
Extinction coefficient	0.004(3)	0.020(5)
Largest diff. Peak and hole	0.300 and −0.240 eÅ ⁻³	1.967 and −1.768 eÅ ⁻³

forms H-bonds with N(3) and N(4) atoms of neighboring cation (O(1)⋯H(B)–N(3) and O(1)⋯H(B)–N(4)). The interaction of amino groups of guanidyl group with the same oxygen atom of the carboxylate group was designated as type *C* [19]. So, in the structure of L-arginine chlorate, both types of interactions, *B* and *C* take place. Due to type *C* interactions, a chain of cations along the *c*-axis is formed, while the connection via type *B* forms cation layers perpendicular to the *a* axis. One more difference is that the O(2) oxygen atom forms an intramolecular H-bond

N(1)–H(A)⋯O(2). As a result, a five-member pseudo-cycle with conformation of highly flattened semi chair is formed by the atoms HA(N1), N(1), C(2), C(1) and O(2), in which the C(2) and N(1) atoms are displaced from the plane, formed by the remaining atoms, by 0.13 and −0.07 Å, respectively.

Let us now consider the arrangement of anions in both structures and their connection with cations. The presence of crystallographically equivalent ClO₃[−] ions in the structure of L-Arg.HClO₃ and two crystallographically independent

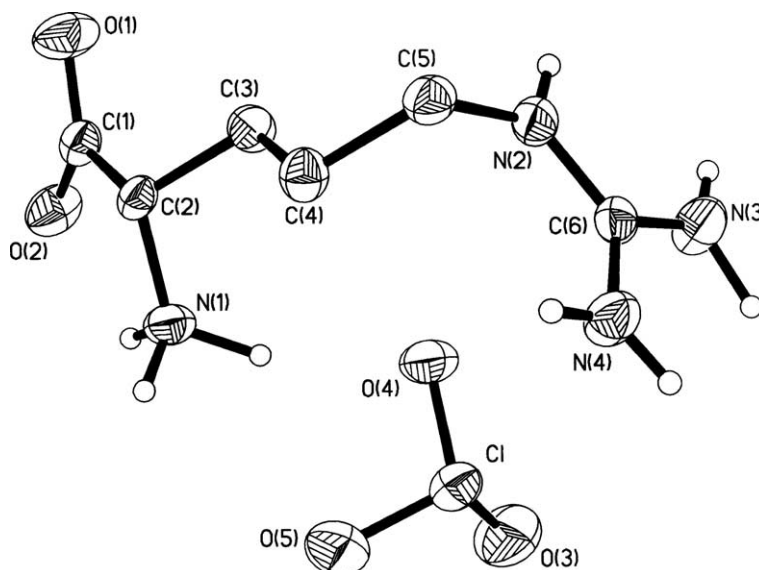


Fig. 4. Independent part of unit cell and numbering of atoms of L-Arg·HClO₃ crystals.

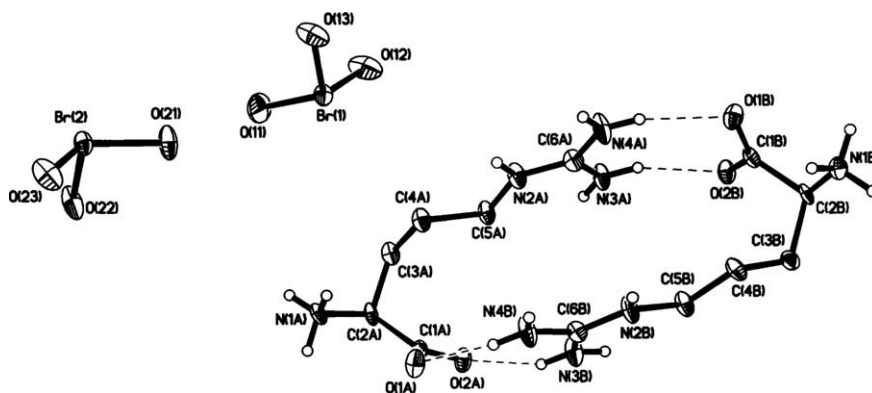


Fig. 5. Independent part of unit cell and numbering of atoms of L-Arg·HBrO₃ crystals.

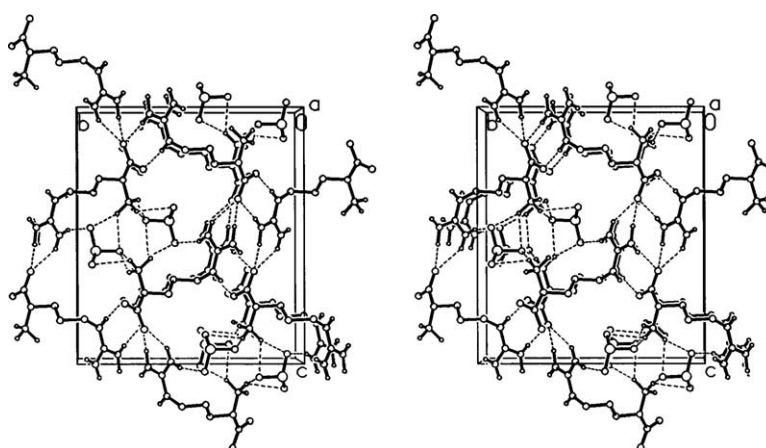


Fig. 6. A stereoscopic view of packing in the crystal structure of L-Arg·HClO₃.

Br(1)O₃⁻ and Br(2)O₃⁻ ions in the structure of L-Arg·HBrO₃ is consistent with the NQR data at 77 K. The average values of Cl–O bond lengths and O–Cl–O angles in the L-Arg·HClO₃ are equal to 1.475 Å and 106.5°, which are characteristic for the ClO₃⁻ ion [20]. The average values of Br(1)–O bond lengths and O–Br(1)–O angles (1.641 Å and 104.4°, respectively) and those for Br(2)O₃⁻ (1.651 Å and 104.6°, respectively) are characteristic of the BrO₃⁻ ion

[20]. In addition to electrostatic interaction, the cations of arginine are connected to anions via H-bonds and ones formed by bromate-ions are stronger than those formed by chlorate-ions. Each of the bromate-ions forms five H-bonds. The Br(1)O₃⁻ ion forms four H-bonds with hydrogen atoms of cation B and one H-bond with cation A, while Br(2)O₃⁻ forms four H-bonds with cation A and one with cation B (Table 7). The ClO₃⁻ anion forms six H-bonds of O···H–N

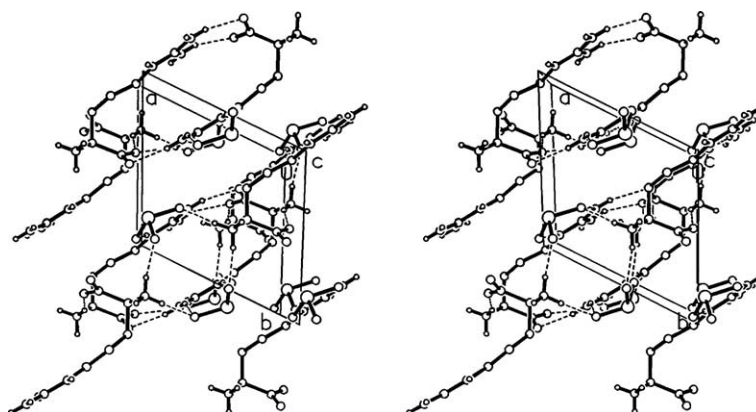


Fig. 7. A stereoscopic view of packing in the crystal structure of L-Arg·HBrO₃.

Table 4
Bond lengths [Å] and angles [°] for L-Arg·HClO₃

Cl(1)–O(3)	1.456(3)	O(3)–Cl(1)–O(4)	106.6(2)
Cl(1)–O(4)	1.481(2)	O(3)–Cl(1)–O(5)	106.6(2)
Cl(1)–O(5)	1.487(3)	O(4)–Cl(1)–O(5)	106.2(2)
C(1)–O(1)	1.239(3)	O(1)–C(1)–O(2)	127.0(3)
C(1)–O(2)	1.241(4)	O(1)–C(1)–C(2)	116.5(3)
N(1)–C(2)	1.501(4)	O(2)–C(1)–C(2)	116.5(2)
N(2)–C(5)	1.453(4)	C(6)–N(2)–C(5)	124.1(3)
N(2)–C(6)	1.329(3)	N(1)–C(2)–C(3)	111.0(2)
N(3)–C(6)	1.328(4)	N(1)–C(2)–C(1)	108.3(2)
N(4)–C(6)	1.328(4)	N(2)–C(5)–C(4)	113.6(3)
C(1)–C(2)	1.545(4)	N(3)–C(6)–N(4)	118.7(3)
C(2)–C(3)	1.523(4)	N(3)–C(6)–N(2)	119.6(3)
C(3)–C(4)	1.520(4)	N(4)–C(6)–N(2)	121.7(3)
C(4)–C(5)	1.524(4)	C(1)–C(2)–C(3)	114.6(2)
		C(2)–C(3)–C(4)	112.7(2)
		C(3)–C(4)–C(5)	113.4(3)

type (Table 6). All of these H-bonds, except O(4)⋯H(C)–N(1), are very weak. According to the Zefirov's H-bond existence criterion [21] the O⋯H contacts lying in the range of 2.15–2.45 Å correspond to the region of most strong van der Waals and most weak hydrogen bonds, and only distances shorter than 2.15 Å definitely correspond to hydrogen bonds. Among H-bonds formed by

the bromate-ions, only one fits the intermediate region. In addition to three covalent bonds, bromine atoms form also secondary bonds. The Br(1)O₃[−] and Br(2)O₃[−] ions differ from each other in this respect. The environment of the Br(1) atom is made up of O(1B), O(2B) and O(22) atoms at the distances 3.243, 3.223 and 3.143 Å, respectively, all shorter than the sum of the van der Waals radii (3.26 Å)

Table 5
Intramolecular bond lengths (and selected intermolecular distances) [Å] and angles [°] for L-Arg·HBrO₃

Br(1)–O(11)	1.635(6)	O(11)–Br(1)–O(13)	107.6(4)
Br(1)–O(12)	1.650(6)	O(11)–Br(1)–O(12)	103.3(4)
Br(1)–O(13)	1.637(6)	O(12)–Br(1)–O(13)	102.3(3)
Br(2)–O(21)	1.662(5)	O(22)–Br(2)–O(21)	105.9(3)
Br(2)–O(22)	1.644(6)	O(22)–Br(2)–O(23)	104.1(3)
Br(2)–O(23)	1.647(5)	O(23)–Br(2)–O(21)	103.9(3)
C(1A)–O(1A)	1.231(9)	O(1A)–C(1A)–O(2A)	126.8(6)
C(1A)–O(2A)	1.271(9)	O(1A)–C(1A)–C(2A)	118.1(6)
N(1A)–C(2A)	1.485(9)	O(2A)–C(1A)–C(2A)	115.1(6)
N(2A)–C(5A)	1.444(9)	N(1A)–C(2A)–C(3A)	111.0(5)
N(2A)–C(6A)	1.333(10)	N(1A)–C(2A)–C(1A)	108.6(5)
N(3A)–C(6A)	1.327(10)	N(2A)–C(5A)–C(4A)	111.3(6)
N(4A)–C(6A)	1.319(11)	N(3A)–C(6A)–N(4A)	119.9(7)
C(1A)–C(2A)	1.532(9)	N(3A)–C(6A)–N(2A)	119.7(7)
C(2A)–C(3A)	1.521(9)	N(4A)–C(6A)–N(2A)	120.4(7)
C(3A)–C(4A)	1.538(10)	C(1A)–C(2A)–C(3A)	111.8(5)
C(4A)–C(5A)	1.532(10)	C(2A)–C(3A)–C(4A)	115.0(6)
C(1B)–O(1B)	1.234(9)	C(3A)–C(4A)–C(5A)	111.4(6)
C(1B)–O(2B)	1.282(9)	O(1B)–C(1B)–O(2B)	125.1(7)
N(1B)–C(2B)	1.498(8)	O(1B)–C(1B)–C(2B)	119.4(6)
N(2B)–C(5B)	1.457(10)	O(2B)–C(1B)–C(2B)	115.5(6)
N(2B)–C(6B)	1.344(9)	C(6B)–N(2B)–C(5B)	122.8(6)
N(3B)–C(6B)	1.319(10)	N(1B)–C(2B)–C(3B)	109.4(6)
N(4B)–C(6B)	1.323(10)	N(1B)–C(2B)–C(1B)	110.4(5)
C(1B)–C(2B)	1.509(10)	N(2B)–C(5B)–C(4B)	109.9(6)
C(2B)–C(3B)	1.525(9)	N(3B)–C(6B)–N(4B)	120.6(7)
C(3B)–C(4B)	1.540(10)	N(3B)–C(6B)–N(2B)	120.4(7)
C(4B)–C(5B)	1.525(10)	N(4B)–C(6B)–N(2B)	119.0(7)
Br(1)⋯O(1b) ⁱ	3.243(6)	C(1B)–C(2B)–C(3B)	112.1(5)
Br(1)⋯O(2b) ⁱ	3.223(5)	C(2B)–C(3B)–C(4B)	112.9(6)
Br(1)⋯O(22) ⁱⁱ	3.143(6)	C(3B)–C(4B)–C(5B)	110.5(6)
Br(2)⋯O(1a) ⁱⁱⁱ	2.881(6)		

Symmetry codes: (i) 1+x,1+y,1+z; (ii) −1+x,−1+y,−1+z; (iii) 1+x,y,1+z

Table 6

The geometric parameters [\AA , $^\circ$] of D–H \cdots A (D-donor, A-acceptor) H-bonds in L-Arg·HClO₃

D–H \cdots A	Symmetry code of A	D \cdots A (\AA)	D–H (\AA)	H \cdots A (\AA)	D–H–A ($^\circ$)
N(1)–H(A) \cdots O(2)	x, y, z	2.604(3)	0.86(5)	2.06(4)	121(3)
N(1)–H(A) \cdots O(5)	$x, -y+0.5, -z$	3.046(4)	0.86(5)	2.38(5)	134(3)
N(1)–H(B) \cdots O(5)	$x+0.5, -y+0.5, -z$	3.033(4)	0.95(4)	2.17(4)	150(3)
N(1)–H(B) \cdots O(3)	$x+0.5, -y+0.5, -z$	3.047(4)	0.95(4)	2.40(4)	125(3)
N(1)–H(C) \cdots O(4)	x, y, z	2.952(4)	1.06(4)	1.92(4)	163(3)
N(1)–H(C) \cdots O(5)	x, y, z	3.092(4)	1.06(4)	2.32(4)	129(3)
N(2)–H(2) \cdots O(2)	$-x-1, y-0.5, -z-0.5$	2.838(3)	0.86(4)	1.98(4)	175(4)
N(3)–H(A) \cdots O(1)	$-x-1, y-0.5, -z-0.5$	2.919(4)	0.81(4)	2.11(4)	176(4)
N(3)–H(B) \cdots O(1)	$-x-0.5, -y, z+0.5$	2.881(4)	1.04(4)	1.90(4)	156(4)
N(4)–H(A) \cdots O(4)	$x+1, y, z$	3.087(4)	0.85(4)	2.27(4)	160(4)
N(4)–H(B) \cdots O(1)	$-x-0.5, -y, z+0.5$	3.000(4)	0.88(4)	2.22(4)	148(4)
N(1)–H(C) \cdots Cl	x, y, z	3.653(3)	1.06(4)	2.63(4)	161(3)
N(1)–H(B) \cdots Cl	$x+0.5, -y+0.5, -z$	3.657(3)	0.95(4)	2.78(4)	153(3)

Table 7

The geometric parameters [\AA , $^\circ$] of D–H \cdots A (D-donor, A-acceptor) H-bonds in L-Arg·HBrO₃

D–H \cdots A	Symmetry code of A	D \cdots A (\AA)	D–H (\AA)	H \cdots A (\AA)	D–H–A ($^\circ$)
N(1A)–H(A) \cdots O(13)	$x, y+1, z$	2.954(8)	0.89	2.10	160
N(1A)–H(B) \cdots O(21)	$x, y, z-1$	2.856(8)	0.89	2.02	155
N(1A)–H(C) \cdots O(2B)	$x+1, y+1, z+1$	2.787(8)	0.89	1.96	155
N(2A)–H(B) \cdots O(22)	$x-1, y-1, z-1$	2.926(8)	0.86	2.07	175
N(3A)–H(D) \cdots O(23)	$x-1, y-1, z-2$	2.947(9)	0.86	2.11	163
N(3A)–H(C) \cdots O(2B)	x, y, z	2.843(8)	0.86	2.02	161
N(4A)–H(C) \cdots O(1B)	x, y, z	2.897(9)	0.86	2.05	167
N(4A)–H(D) \cdots O(21)	$x-1, y-1, z-1$	2.975(9)	0.86	2.12	171
N(1B)–H(A) \cdots O(11)	$2-x, y-1, z-1$	2.831(9)	0.89	2.00	154
N(1B)–H(B) \cdots O(2A)	$x-1, y-1, z$	2.751(8)	0.89	1.95	149
N(1B)–H(C) \cdots O(23)	$X-2, y-2, z-2$	2.829(8)	0.89	1.96	165
N(2B)–H(B) \cdots O(12)	$x-1, y, z$	2.853(8)	0.86	2.00	171
N(3B)–H(C) \cdots O(2A)	x, y, z	2.827(9)	0.86	2.01	158
N(3B)–H(D) \cdots O(13)	$x-1, y, z-1$	3.005(9)	0.86	2.15	171
N(4B)–H(C) \cdots O(1A)	x, y, z	2.863(9)	0.86	2.01	172
N(4B)–H(D) \cdots O(11)	$x-1, y, z$	3.115(11)	0.86	2.32	155

[22]. The Br(2) atom forms a secondary bond only with O(1A) atom, but the distance Br(2) \cdots O(1A) being equal to 2.881 \AA , is essentially shorter than that in the preceding case and shorter than the minimum distance 3.04 \AA for the van der Waals interaction between bromine and oxygen atoms [21].

In the ClO₃[−] anion the chlorine atom has no secondary bonds with oxygen atoms at distances close to the sum of van der Waals radii for Cl and O. Instead, the environment of the chlorine atom is made up of two hydrogen atoms from the two closest α -amino groups at distances of 2.633 \AA (Cl \cdots H(N1C) (x, y, z)) and 2.781 \AA (Cl \cdots H(N1B)($0.5+x, 0.5-y, -z$)). The sum of Cl and H van der Waals radii is 3.06 \AA , while the minimum Cl \cdots H distance at their van der Waals interaction is 2.67 \AA . Such a difference in behavior of ClO₃[−] and BrO₃[−] anions may be caused by the difference in electronegativity of chlorine and bromine atoms. Among the Cl, Br and I atoms, the bromine atom is intermediate in electronegativity. Due to the large electronegativity difference between oxygen and iodine, the formal charge on the iodine atom in the IO₃[−] ion is positive [23]. As a result,

the secondary I \cdots O bonds (2.7–2.9 \AA) shorter than the minimum (3.17 \AA by [21]) distance for I \cdots O van der Waals interactions are usual in the structures of iodates. Moreover, the so-called intermediate bonds between the first and second coordination spheres with distances 2.4–2.5 \AA were sometimes observed (see Ref. [24] and references therein). In the ClO₃[−] ion the formal charge on the central atom is negative [23], which may probably explain the absence of Cl \cdots O secondary bonds and the presence of the shortened Cl \cdots H contacts in the structure of L-Arg.HClO₃. In the case of intermediate bromine, the BrO₃[−] ion is more similar to IO₃[−] due to existence of Br \cdots O secondary bonds, whereas its electronic structure is more similar to that of the ClO₃[−] ion with the negative charge less than in the ClO₃[−] ion.

4. Conclusion

Although both salts L-Arg.HClO₃ and L-Arg.HBrO₃ are formed by the same mechanism (L-Arg⁺.ClO₃[−], L-Arg⁺.BrO₃[−]) however, they are not isostructural (space groups:

P2₁2₁2₁ and P1 respectively) and have essential distinctions in crystal packing.

Acknowledgements

The research described in this publication was made possible in part by CRDF Grant No. AE2-2533-YE-03. The piezo- and pyroelectric studies were supported by Russian Foundation of Basic Research, Grant No. 02-02-17798. We thank Dr Martirosyan G.G. for his help in recording the FT-IR ATR spectra. We thank also reviewer for useful comment.

References

- [1] G.C. Bhar, A.V. Rudra, P.K. Datta, U.N. Roy, V.K. Wadhawan, T. Sasaki, *Pramana: J. Phys.* 44 (1995) 45.
- [2] A. Yokotani, T. Sasaki, K. Fujioka, S. Nakai, Ch. Yamanaka, *J. Cryst. Growth* 99 (1990) 815.
- [3] V. Venkataramanan, G. Dhanaraj, H.L. Bhat, *J. Cryst. Growth* 140 (1994) 336.
- [4] G. Dhanaraj, T. Shripathi, H.L. Bhat, *J. Cryst. Growth* 113 (1991) 456.
- [5] J.F. Carvalho, A.C. Hernandez, F.D. Nunes, L.B.O.A. de Moraes, L. Misoguti, S.C. Zilio, *J. Cryst. Growth* 173 (1997) 487.
- [6] G. Arunmozhi, R. Jayavel, C. Subramanian, *J. Cryst. Growth* 178 (1997) 387.
- [7] L. Aidong, X. Chongquan, L. Aiben, M. Naiben, *J. Cryst. Growth* 220 (2000) 291.
- [8] A.S. Haja Hameed, G. Ravi, P. Ramasamy, *J. Cryst. Growth* 229 (2001) 547.
- [9] R. Shanmugavadivu, G. Ravi, R. Jayavel, R. Mohankumar, A. Nixon Azariah, *J. Cryst. Growth* 271 (2004) 252.
- [10] A.M. Petrosyan, R.P. Sukiasyan, H.A. Karapetyan, S.S. Terzyan, R.S. Feigelson, *J. Cryst. Growth* 213 (2000) 103.
- [11] A.S. Haja Hameed, P. Anandan, R. Jayavel, P. Ramasamy, G. Ravi, *J. Cryst. Growth* 249 (2003) 316.
- [12] D. Xu, X.Q. Wang, W.T. Yu, S.X. Xu, G.H. Zhang, *J. Cryst. Growth* 253 (2003) 481.
- [13] K. Vasantha, S. Dhanuskodi, *J. Cryst. Growth* 269 (2004) 333.
- [14] S.B. Monaco, L.E. Davis, S.P. Velsko, F.T. Wang, D. Eimerl, A. Zalkin, *J. Cryst. Growth* 85 (1987) 252.
- [15] A.M. Petrosyan, S.S. Terzyan, V.M. Burbelo, R.P. Sukiasyan, *Z. Naturforschung* 53a (1998) 528.
- [16] G.M. Sheldrick, SHELX86. Program for the solution of crystal structures. University of Göttingen, Germany, 1985.
- [17] G.M. Sheldrick, SHELXL93. Program for the refinement of crystal structures. University of Göttingen, Germany, 1993.
- [18] G.K. Semin, T.A. Babushkina, G.G. Yakobson, *Primenenie yadernogo kvadrupol'nogo rezonansa v khimii*, 'Khimia' Leningrad, 1972; G.K. Semin, T.A. Babushkina, G.G. Yakobson, *Nuclear Quadrupole Resonance in Chemistry*, Wiley, New York, 1975.
- [19] D.M. Salunke, M. Vijayan, *Int. J. Pept. Protein Res.* 18 (1981) 348.
- [20] A.F. Wells, *Structural Inorganic Chemistry*, Fifth ed., Oxford University Press, Moscow, 1986 (Russian edition in vol. 3, (Mir), Moscow).
- [21] Yu.V. Zefirov, *Kristallografiya* 44 (1999) 1091.
- [22] Yu.V. Zefirov, P.M. Zorky, *Uspekhi khimii* 64 (1995) 446.
- [23] B.D. El-Issa, A. Hinchliffe, *J. Mol. Struct.* 67 (1980) 317.
- [24] A.M. Petrosyan, V.A. Shishkin, *Z. Naturforschung*, 51a (1996) 667.